Deep-Sea Research I 94 (2014) 173–183

Contents lists available at ScienceDirect

Deep-Sea Research I

journal homepage: www.elsevier.com/locate/dsri

Oxygen distribution and aerobic respiration in the north and south eastern tropical Pacific oxygen minimum zones

Laura Tiano [a,*], Emilio Garcia-Robledo [a], Tage Dalsgaard [b], Allan H. Devol [c], Bess B. Ward [d], Osvaldo Ulloa [e], Donald E. Canfield [f], Niels Peter Revsbech [a]

[a] Section of Microbiology, Department of Bioscience, Aarhus University, 8000 Aarhus C, Denmark
[b] Arctic Research Centre, Department of Bioscience, Aarhus University, 8000 Aarhus C, Denmark
[c] School of Oceanography, University of Washington, Seattle 98195-7940, WA, USA
[d] Department of Geosciences, Princeton University, NJ, 08544 Princeton, USA
[e] Departamento de Oceanografía & Instituto Milenio de Oceanografía, Universidad de Concepción, 4070386 Concepción, Chile
[f] Nordic Center for Earth Evolution, Institute of Biology, University of Southern Denmark, 5230 Odense M, Denmark

ARTICLE INFO

Article history:
Received 18 July 2014
Received in revised form
30 September 2014
Accepted 1 October 2014
Available online 14 October 2014

Keywords:
Oxygen
Community respiration
Oxygen minimum zone
Eastern tropical Pacific
STOX sensor

ABSTRACT

Highly sensitive STOX O_2 sensors were used for determination of in situ O_2 distribution in the eastern tropical north and south Pacific oxygen minimum zones (ETN/SP OMZs), as well as for laboratory determination of O_2 uptake rates of water masses at various depths within these OMZs. Oxygen was generally below the detection limit (few nmol L^{-1}) in the core of both OMZs, suggesting the presence of vast volumes of functionally anoxic waters in the eastern Pacific Ocean. Oxygen was often not detectable in the deep secondary chlorophyll maximum found at some locations, but other secondary maxima contained up to ~0.4 μmol L^{-1}. Directly measured respiration rates were high in surface and subsurface oxic layers of the coastal waters, reaching values up to 85 nmol L^{-1} O_2 h^{-1}. Substantially lower values were found at the depths of the upper oxycline, where values varied from 2 to 33 nmol L^{-1} O_2 h^{-1}. Where secondary chlorophyll maxima were found the rates were higher than in the oxic water just above. Incubation times longer than 20 h, in the all-glass containers, resulted in highly increased respiration rates. Addition of amino acids to the water from the upper oxycline did not lead to a significant initial rise in respiration rate within the first 20 h, indicating that the measurement of respiration rates in oligotrophic Ocean water may not be severely affected by low levels of organic contamination during sampling. Our measurements indicate that aerobic metabolism proceeds efficiently at extremely low oxygen concentrations with apparent half-saturation concentrations (K_m values) ranging from about 10 to about 200 nmol L^{-1}.

1. Introduction

Oxygen is a fundamental constraint on marine life, and it regulates many biological and chemical processes in the Ocean. Since oxygen is directly linked to carbon by photosynthesis and respiration, it is a diagnostic of the rate at which organic matter cycles in the Oceans (Keeling et al., 2010; Stramma, 2008). Its regulatory role is particularly evident in marine areas like oxygen minimum zones (OMZs) (Paulmier and Ruiz-Pino, 2009), where a combination of natural conditions, such as high productivity surface waters, stratification, and reduced circulation leads to extensive depletion of dissolved oxygen at intermediate depths of the water column (Wyrtki, 1962). The resulting oxygen gradients favor a complex succession of aerobic and anaerobic respiration processes with depth (Wright et al., 2012), that are tightly regulated by local O_2 levels and the presence of electron donors and alternative electron acceptors. The presence of OMZ regions was described in the early 1900s (Schmidt, 1925) and during recent decades their biogeochemical importance has been recognized, as they are estimated to account for 21–39% of the global oceanic nitrogen (N) loss and a similar percentage of oceanic N_2O emission (Bange, 2006; DeVries et al., 2012a; Kalvelage et al., 2013). Only recently we have gained the technical ability to resolve the O_2 distribution in the OMZ with satisfactory accuracy, and to determine the effect of nanomolar O_2 concentrations on biogeochemical cycling. Our ability to detect in situ oxygen concentration in the OMZ improved by about three orders of magnitude, as we progressed from the traditionally used Winkler titrations or electrochemical and optode sensors having detection limits around 1–2 μmol L^{-1}, to the Switchable Trace Oxygen (STOX) microsensor, that has a detection limit in the range of 1–10 nmol L^{-1} (Revsbech et al., 2009). The STOX sensor is an oxygen microsensor with front guard cathode,

* Corresponding author. Tel. +45 60286466.
E-mail address: tiano.laura@gmail.com (L. Tiano).

http://dx.doi.org/10.1016/j.dsr.2014.10.001

which enables in situ zero calibration, thus allowing measurement of near zero oxygen concentrations. Consequently the eastern tropical south Pacific (ETSP) OMZs as well as the OMZ in the Arabian Sea were renamed Anoxic Marine Zones (AMZs) (Ulloa et al., 2012), because no O_2 could be detected in the water layers occurring between 20 and 100 m depth and down to a few hundred meters depth. These totally anoxic water layers were shown to coincide with extensive NO_2^- accumulation (Canfield et al., 2010; Jensen et al., 2011; Thamdrup et al., 2012). Recent investigations have reported that the transitions between aerobic and anaerobic respiration in OMZs are regulated by O_2 levels in the nanomolar range. Even O_2 concentrations as low as 1 μmol L^{-1} or less appear to be inhibitory for anaerobic ammonium oxidation (anammox) and, to higher extent, for denitrification (Dalsgaard, personal communication); in addition both oxidations of ammonium and nitrite (Bristow, unpublished data) exhibit very low half-saturation concentrations for O_2 and these oxidation processes may occur at much lower oxygen concentrations than previously anticipated.

Forecasted decline in Ocean dissolved O_2 (Ocean deoxygenation) will likely lead to expansion, in area and volume of OMZs with widespread consequences (Keeling et al., 2010). Thus there is a need for more detailed data on the current O_2 distribution, dynamics and consumption rates in OMZ and AMZ waters, with focus on process regulation at low O_2 concentrations.

In this study we investigated the depth and regional variation of oxygen concentration, aerobic respiration in low oxygenated waters, and the potential for aerobic respiration in anoxic waters from the eastern tropical north and south Pacific (ETNP-ETSP) OMZs, through a combination of high sensitivity in situ and laboratory based STOX sensor measurements.

2. Material and methods

2.1. Experimental area and sampling

A total of three stations were investigated during two cruises in two main experimental areas: the eastern tropical north Pacific (ETNP) and the eastern tropical south Pacific (ETSP) (Fig. 1).

During the ETNP Spring Cruise (March and April 2012) aboard the R/V Thomas G. Thompson experiments were carried out at two main stations: one about 50 km from the Mexican coast, M1 (N 20° 03′ 50, W 106° 00′ 81), and an oceanic one (~700 km from the Mexican coast) M2 (N 16° 29′ 93, W 109° 59′ 00) (Fig. 1). In addition dissolved oxygen distribution was determined in two transects (Fig. 2 and S3). Profiles of physical variables were registered with a Seabird SBE-911 conductivity–temperature–depth (CTD) system, which was equipped with an SBE 43 oxygen sensor and an in situ STOX sensor unit (Unisense A/S). Seawater samples were collected using a 10-L Niskin bottle rosette.

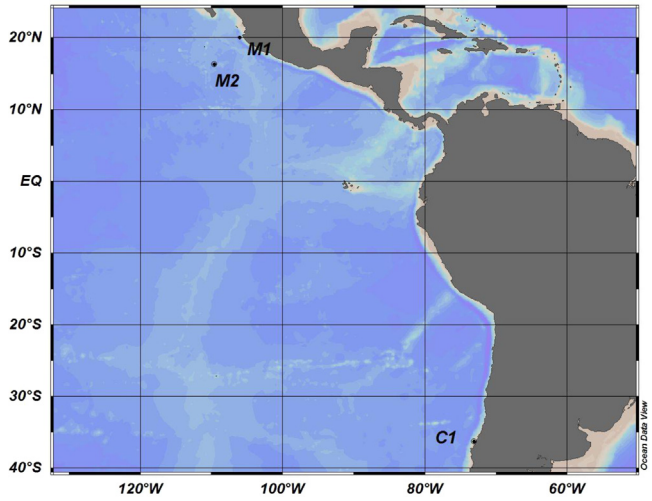

Fig. 1. *Map of the study area and sampling stations*. Study areas were located in the eastern tropical north and south Pacific, with three main sampling stations: M1, coastal Mexico; M2, off shores Mexico; C1, off Dichato, central Chile (Ocean Data View).

In the ETSP, Station C1 (S36°30′85, W73°07′75), ~18 km from the coast, was sampled during the MOOMZ4 cruise (March 2012) off Chile, using a pump profiling system (PPS) equipped with a Seabird SBE-25 CTD with an SBE 43 oxygen sensor package and an in situ STOX unit. Incubations were carried out in the Dichato laboratories of Universidad de Concepción.

High resolution oxygen profiling with the STOX sensor (Revsbech et al., 2009; Revsbech et al., 2011) was typically carried out on the first cast, together with nutrient measurements (Fig. S4), to characterize the water column at each station. We selected the depths for sampling mainly on the basis of in situ oxygen concentrations, detected by the STOX sensor and the two SBE 43 oxygen sensors, targeting seawater masses with naturally different oxygen concentrations. The main chosen primary sample depths were: oxygenated surface waters, partially oxygen depleted oxycline waters and completely oxygen depleted waters from below the oxycline. For each depth bottle incubations were performed shortly after sampling, as shown below.

2.2. Reactor experiments and STOX sensor

2.2.1. Measurements of community respiration rates

Experiments from stations M1, M2 and C1 were carried out in custom-modified Schott Duran® glass bottles of 1160 mL. The bottle design and filling procedure has been described previously (Tiano et al., 2014). During the incubations the bottles were kept in darkness and submersed in a water bath maintained at the desired temperature (12 °C for C1; 14 °C for M1 and M2). Continuous stirring was accomplished using glass coated magnets (Fisher Scientific®), while placing the container with the bottles on magnetic stirrers (IKA®). The seawater was partially or fully degassed by constant bubbling with He (Station C1) or N_2+0.04% CO_2 (stations M1 and M2) before being siphoned into the incubation bottles under a stream of N_2. If O_2 concentrations were too low for the specific experiment small volumes of water were added by a syringe with a long needle through the pressure compensation tube of the bottle. All experiments were conducted within 24 h of sampling with incubations for respiration rates normally lasting ~15 h. Before all experiments the glassware was washed in 0.1 M NaOH and subsequently in 0.1 M HCl to avoid organic contamination.

The STOX microsensors were built as described previously (Revsbech et al., 2009; Revsbech et al., 2011). Calibration was performed by injecting known volumes of air-saturated water into each bottle. The electronics applied for shipboard and laboratory based experiment were identical. The sensor currents were measured with a PA8000 eight-channel picoammeter (Unisense A/S), while the polarization and depolarization of the front guard were regulated by a custom-built timer-controlled switch-box with the timer set to cycles of 200 s on and 200 s off. The signals were collected by a Unisense ADC816 16-bit A/D converter, connected to a portable PC using the program Sensortrace Basic (Unisense A/S).

2.2.2. Effects of organic contamination and time on community respiration rates

Two sets of experiments were performed in order to investigate the effects of time (i) and organic contamination (ii) on CR rates in discrete bottle incubations. i) The effect of time solely was evaluated on water samples from 900 m depth that were incubated in two reactors for a total time of 37 h. ii) Organic

contamination was simulated with amendment of casamino acids to the samples. A solution of casamino acids, source of both carbon and nitrogen, was injected into two bottles containing seawater from 102 m depth to a final concentration of 1 mg L^{-1}. The time course of O_2 consumption in both amended and two unamended bottles, was monitored over an extended time frame of 60 h.

2.3. Data analysis

Data processing was done in Microsoft Excel. Respiration rates were calculated by simple linear regression of oxygen concentration versus incubation time over discrete ranges of oxygen concentrations and the fit to a linear model was evaluated by the

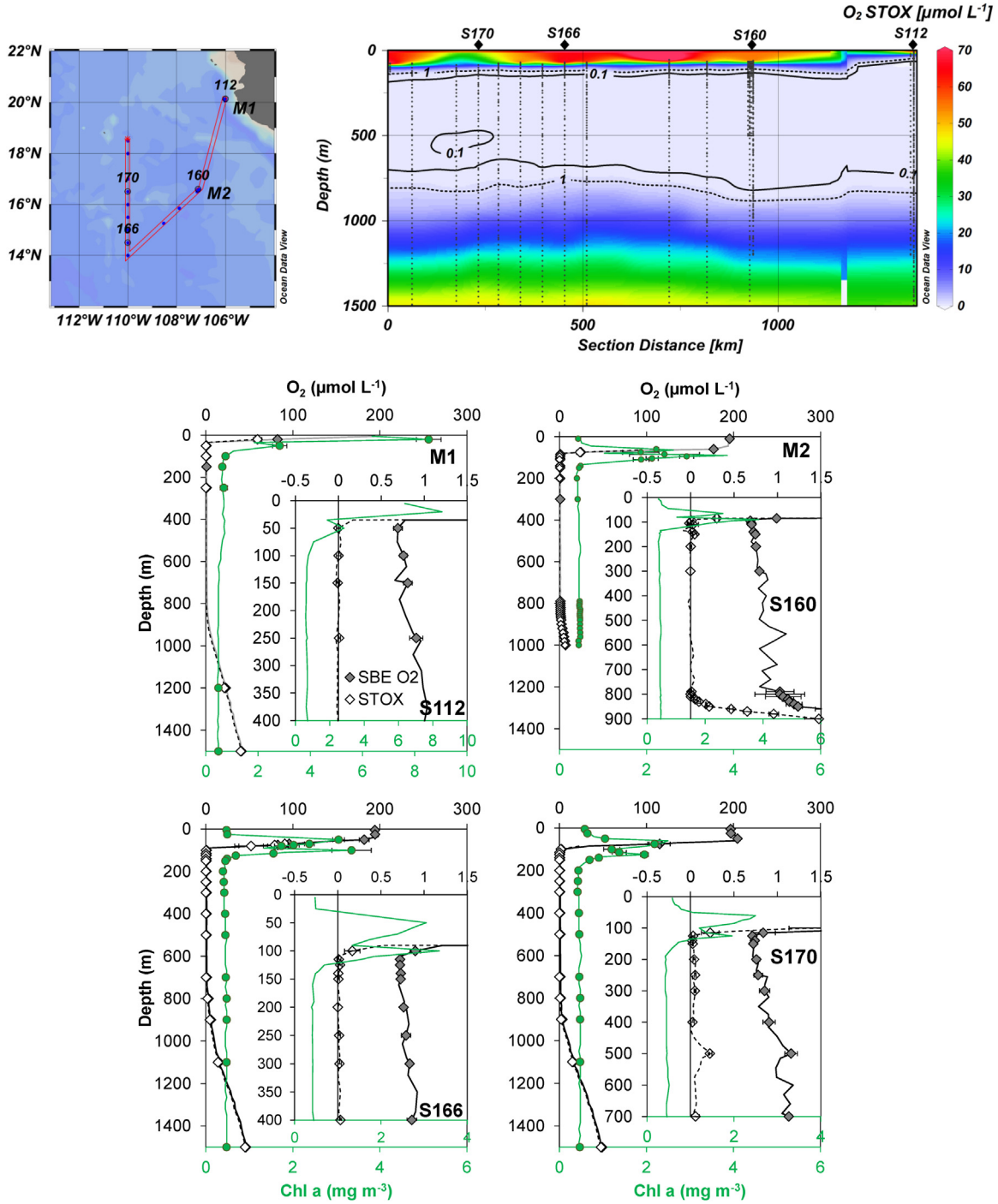

Fig. 2. *ETNP: map of the study area, spatial O_2 distribution and representative casts.* The map is showing the main stations in the ETNP: M1 and M2, and the two transects (up-left corner). The oxygen distribution measured with the STOX sensors, along the red-marked transects, is represented as a contour plot (up-right corner). Below four representative upward casts are shown: 170, 166, 160 (from St. M2) and 112 (from St. M1). In the upward casts figures, dots are used for data recorded when the sensors remained at a fixed depth (mean concentration ± SD, n=5–9), whereas lines are used to represent the data measured while the CTD was moving. Depth distribution of oxygen is shown by open diamonds (◇), when measured by the STOX sensor, and with gray diamonds (◆), when measured by the SBE43. Chlorophyll *a* profiles are shown with green circles (●). For comparison purposes, data from the SeaBird sensors were averaged over the duration of the STOX cycles, resulting in the same number of data points as the STOX measurements. The inserts show the same casts amplified over the depths of the upper oxycline. For the STOX sensor, the variation, shown by SD bars at the depths of the oxycline, reflects actual temporal fluctuations in the oxygen concentration during the measurement. The average resolution (± SD) through the OMZ cores for the presented casts was: M1 (between 50 and 750 m) 4 ± 18 nmol L^{-1} O_2 and M2 (between 125 and 650 m) 27 ± 39 nmol L^{-1} O_2.

correlation coefficient, r^2, all rates presented have $R^2 > 0.60$. When possible kinetic parameters: V_{max} (maximum respiration rate) and K_m (apparent half-saturation concentration) for community respiration (CR) were estimated using a modified equation from an empirical relationship, originally developed for light saturation curves for photosynthesis (Jassby and Platt, 1976) as described previously (Tiano et al., 2014).

2.4. In situ oxygen profiling

High resolution in situ oxygen data were acquired with a STOX sensor unit as described by Revsbech et al. (2011). Sensors were operated with 10 s front guard cathode polarization, 20 s front guard depolarization cycles, and data were logged by the Seabird CTD electronics at a rate of 24 s^{-1}. The amplification of the signal was set so that the highest oxygen concentrations close to the surface were out of range, as the 12-bit AD converter of the Seabird CTDs otherwise would result in an insufficient resolution of low O_2 concentrations. The calibration of the in situ STOX sensor was done using paired values of STOX signal and oxygen concentration signal and oxygen concentration measured by the SBE 43 sensors at depths where O_2 concentrations were relatively high but still below the maximum of the STOX electronics. We did not compensate for the rather small effect of pressure found at water depths of less than 1000 m (a decrease in sensitivity of 3% can be expected at 500 m according to Glud et al. (2000), but it was necessary to compensate for sensitivity changes due to temperature).

Calibrations done on 4 different sensors showed the following relationship:

$$\text{Signal } \% = (31.9 + 2.72 \times T)\% \quad (1)$$

where Signal % is the percentage of the signal at 25 °C obtained at a temperature of T °C.

Oxygen concentrations were analyzed with the STOX sensors during the upcasts, where both SBE43 and STOX sensors are more stable, and the release of oxygen from polymers in the Seabird instruments should be minimized (see Supplementary Material). Data, used for the calculation of accurate values and the detection limit for oxygen for each station were collected at depths where water was sampled, and the CTD therefore was positioned for several minutes. In situ detection limit during the deployments varied from 4 to 300 nmol L^{-1} O_2 due to differences in the resolution of the electronic units and quality of the sensors used during the different cruises.

2.5. Nutrient analysis

Nutrient samples were analyzed on board (ETNP cruise). Water samples were filtered (GFF glass fiber) before analysis, and analyzed using the US-JGOFS protocols (http://usjgofs.whoi.edu/protocols_rpt_19.html). Nutrient samples for the ETSP cruise

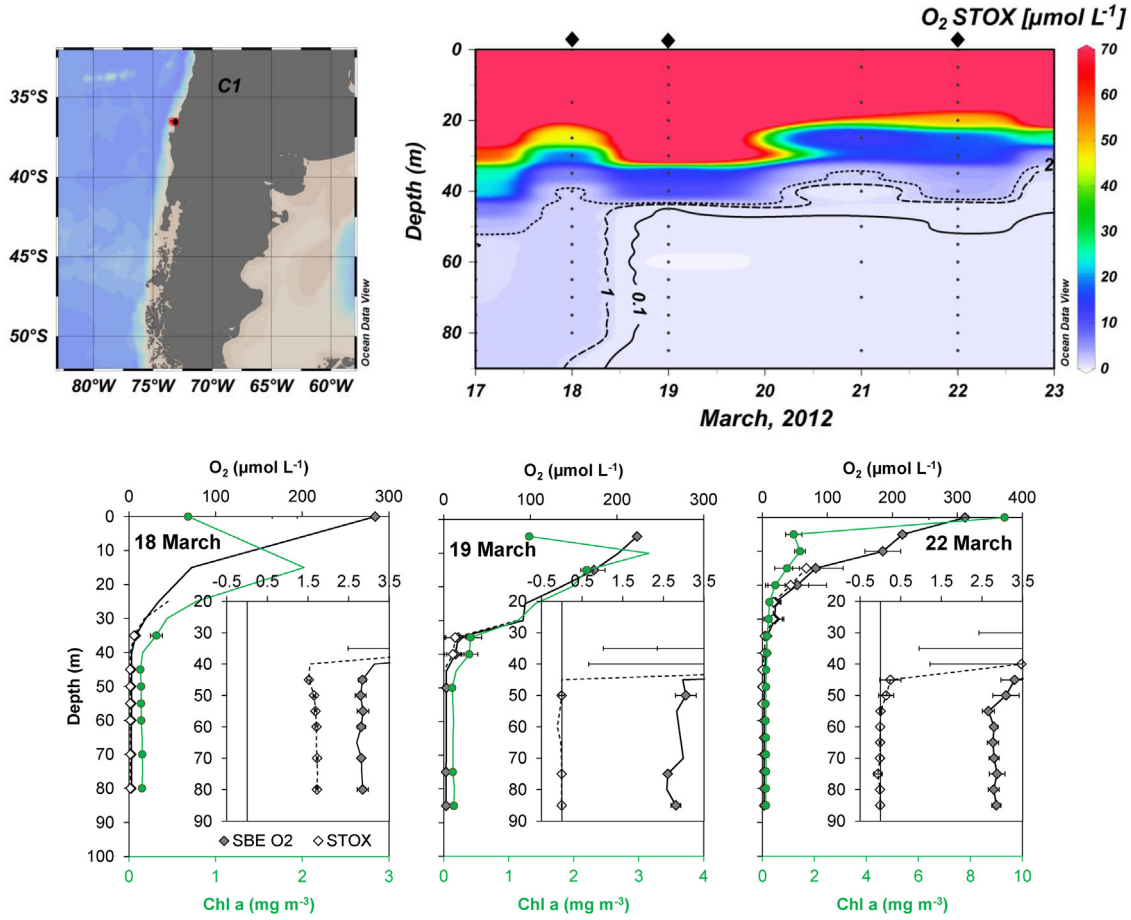

Fig. 3. *ETSP: map of the study area, time evolution of O_2 distribution, and representative casts.* The map is showing the station in the ETSP: C1 (up-left corner). The oxygen concentration evolution, measured by the STOX sensor, during the experimental period is then represented as a contour plot (up-right corner). Below three representatives upward casts from different days are shown. Depth distribution of oxygen is shown by open diamonds (◇), when measured by the STOX sensor, and by gray diamonds (◆), when measured by the SBE43. Chlorophyll *a* profiles are shown with green circles (●). In the figure dots are used for data recorded when the sensors remained at a fixed depth (mean concentration ± SD, n=5–9). Whereas lines are used to represent the data measured while the CTD was moving. The inserts show the same casts amplified over the depths of the upper oxycline. The average resolution (±SD) through the OMZ core (between 50 and 85 m) for the presented casts was 20 ± 32 nmol L^{-1} O_2.

were analyzed in a land-based laboratory using standard procedures (for representative in situ nutrients profiles and hydrocasts see Fig. S4).

3. Results

3.1. In situ oxygen distribution in the ETNP and ETSP OMZs

For all the investigated stations (M1, M2 and C1) (Fig. 1), and during two transects in the ETNP (Figs. 2 and S3) oxygen was consistently below detection limit of the STOX sensors in both ETNP and ETSP OMZ cores (Figs. 2 and 3).

From the near-shore Station M1, located ~50 km from the Mexican coastline, to the open Ocean Station M2 (~700 km), the thickness of the completely oxygen depleted water layers decreased, as the depth of the upper oxycline increased, from 15–25 m at M1 to 100–150 m at M2 (Fig. 2). Less variability was found for the position of the lower oxycline where deep oxygenated waters appeared around 700–800 m depth. At the upper oxycline the oxygen concentration often changed abruptly over a span of a few meters, from near saturation to below detection limit, whereas the lower oxycline was characterized by less steep concentration gradients. In Fig. 2, Cast 160 represents an example of micro-oxic conditions over a larger depth interval. A 70 m thick zone from 810 to 880 m depth was found to have O_2 concentrations between 5 and 957 nmol O_2 L^{-1}. Other casts showed layers with sub-micromolar O_2 concentrations surrounded by hundreds of meters of anoxic water. Cast 170 (Fig. 2, Table 1) had a ~130 m thick oxic layer with a maximum concentration of 0.224 ± 0.009 μmol L^{-1} at 500 m depth, with adjacent anoxic water masses down to 720 m and up to 115 m. Cast 171, located at 82 km from Cast 170, had a similar layer of oxic water from 475 to 620 m with maximum concentrations of 143 ± 19 nmol L^{-1} here with anoxia from 705 to 620 m and from 475 to 105 m. The extent of the oxic water masses may be slight underestimated, as the applied STOX sensor and associated electronics only exhibited a resolution of 70 nmol L^{-1} per AD count at an in situ temperature of 8 °C. Oxic water causing less than about half an AD count (35 nmol L^{-1}) could thus go undetected.

Station C1 (Figs. 1–3), off Dichato, was analyzed at the end of the austral summer when the seasonal OMZ, which is an extension of the permanent ETSP OMZ, was still present. Oxygen decreased continuously from the water surface down to the oxic–anoxic interface at 40–50 m, and O_2 was below detection (about 10 nmol L^{-1}) down to the bottom (about 100 m depth) for the majority of the period. A high degree of mixing and variability was detected at station C1 during the period of investigation, as visible in Fig. 3. The upper limit of the anoxic layer (0.1 μmol L^{-1} isoline) varied between days, oscillating between 45 and 55 m. During 17th and 18th of March, the core of the OMZ was not anoxic and concentrations between 1 and 2 μmol L^{-1} were measured (Table 1).

3.2. In situ oxygen concentration in the ETNP OMZ secondary chlorophyll maximum

A secondary chlorophyll *a* maximum was detected at both Stations M1 and M2 (~50 m and 110 m depth, respectively), whereas no such feature was detected at Station C1 in the ETSP OMZ at the time of this study. In the first case, the secondary chl maximum was below the upper oxycline and no O_2 was detectable in those waters (O_2 resolution with a relatively poor STOX sensor ~200–300 nmol L^{-1}) (Fig. 2, Cast 112). For Station M2, 5 casts out of 6 showed that the approximately 10–50 m thick water layer containing the secondary maximum contained O_2 concentrations in the low nanomolar range (up to 400 nmol L^{-1}, O_2 resolution ~28 nmol L^{-1}) (Fig. 2, Cast 160). Another example of the presence of oxygen at the secondary chlorophyll maximum can be seen in the Cast 166, where the average O_2 concentration ± SE (n) at 100 m was 168 ± 18 (5) nmol L^{-1} (Fig. 2, Cast 166). Cast 147 showed an O_2 concentration in the secondary chlorophyll maximum of 66 ± 13 (6) nmol L^{-1}, at this location the photosynthetically active radiation (PAR) was also measured. The PAR at secondary chlorophyll maximum depth (110 m) was 0.75 μE/m^2 s, whereas at the first chlorophyll maximum (55 m depth) it was 58.9 μE/m^2 s (around 16.00–17.00 UTC). Detailed in situ data showing an oxic secondary chlorophyll maximum (cast 158) are shown in Fig. S1.

Table 1
Oxygen concentration measured with STOX sensors in the representative upward casts from ETNP and ETSP. The table shows oxygen concentrations from representative upward casts presented in Fig. 2, off Mexico (S112, S160, S166, S170), and in Fig. 3 off Chile (days 18, 19 and 22 of March). Measurements (mean ± SE) were taken while the sensor was standing at a fixed depth in order to register several polarization cycles (number of cycles in brackets). Values shown for the anoxic core (between 200 and 500 m in north Pacific and below 50 m in the south Pacific) could be considered as the detection limit for that sensor at that station, except for the S170 at 500 m (*) where an intrusion of oxygen locally increased the measured concentration (see Fig. 2).

Depth (m)	**O_2 (nmol L^{-1})**			
	S112	**S160**	**S166**	**S170**
100	3 ± 9 (9)	28 ± 28 (5)	168 ± 40 (5)	1627 ± 201 (6)
200–300	9 ± 6 (7)	2 ± 5 (7)	1 ± 1 (5)	43 ± 6 (5)
500			60 ± 19 (5)	224 ± 9 (6)*
800		0 ± 0 (4)	1869 ± 6 (5)	675 ± 1 (5)
	March 18	**March 19**		**March 22**
40–45	1522 ± 10 (25)	10629 ± 779 (164)		3467 ± 121 (345)
50	1653 ± 4 (62)	−4 ± 21 (10)		142 ± 10 (346)
60	1709 ± 8 (21)			−7 ± 1 (347)
80–85	1721 ± 6 (23)	−3 ± 1 (221)		−4 ± 1 (348)

3.3. Bottle incubation experiments and oxygen uptake rates

3.3.1. Community respiration: regional and depth variations

The respiration rates at each sampled depth of the four stations are presented as averages of O_2 uptake rates expressed in a diverse range of oxygen concentrations, as shown in Table 2, and for Stations M1 and C1 also presented graphically in Fig. 4.

As a general trend, higher respiration rates were found in oxic surface waters (up to 70 nmol L^{-1} h^{-1}, St. C1) (Table 2, column 2) and in the deep oxygenated waters (below 800 m) very low rates were detected. The rates obtained for M1 at 1200 m were as high as 3.3 nmol L^{-1} h^{-1}, but this can be considered as an artifact due to the rather high O_2 concentration at which the sample was incubated and therefore poor resolution was applied to the measurements. Deep water from Station M2 was incubated at about 150 nmol L^{-1} O_2 and exhibited apparent respiration rates of 0.2 nmol L^{-1} h^{-1}. This is probably also an overestimate, as we are approaching the detection limit of the STOX sensor at the applied O_2 concentration, and the real respiration rate may have been only a small fraction of this number. For Station M1 the highest respiration rate was found at 10 m (88 nmol L^{-1} O_2 h^{-1}) along with a chlorophyll maximum, whereas rates in waters at the upper oxycline and just below the upper oxycline were around one third of that, decreasing drastically when entering the OMZ anoxic core, and with increasing depth. A good correlation (R^2=0.8) was found between the community respiration (CR) and beam transmission values. Beam transmission in surface waters was inversely related to the fluorescence. Nevertheless, fluorescence exhibited an overall poor correlation with CR (R^2=0.5), due to the secondary chlorophyll maximum at 40 m, where high chlorophyll concentration was present in waters with low CR. Station M2, open Ocean

Table 2
Average respiration rates, chlorophyll a and beam transmission values for the sampling stations. Average respiration rates for sampled depths from bottle incubations, and chlorophyll *a* and beam transmission values for the sampled water masses, are presented in the table. Column 1 presents the respiration rates as average values. Averages were calculated over the O_2 range presented, number of values included in the average (n) ± SD. Samples were incubated at diverse O_2 ranges in replicate bottles filled from a common reservoir. Column 2 "Respiration rate*" presents more comparable respiration rates (n) ± SD, calculated as averages of rates expressed when samples were incubated in the O_2 concentration range: 2500–600 nmol L^{-1} O_2, (na – data not available).

Station	Depth (m)	Incubation O_2 range (nmol L^{-1} O_2)	OMZ layer	1. Resp. rate (nmol O_2 L^{-1} h^{-1}) (n)	2. Resp. rate* (nmol O_2 L^{-1} h^{-1}) (n)	Chl (mg/m^3)	Beam transmission (%)
M1	4	2400–30	Oxic	41.8 (5) ± 10.3	32(2)	1.7	87.08
	10	4000–3000	Oxic	84.7 (3) ± 9.5	na	5.01	81.63
	25	4500–200	Oxycline	33.5 (4) ± 5.9	39 (1)	1.76	96.55
	30	1700–0	Oxycline	33.3 (7) ± 18	42 (3) ± 11	0.52	99.64
	40	2200–1000	Sec chl. max	26.0 (3) ± 8.5	26 (3) ± 9	4.14	95.8
	300	2000–150	Below oxycline	5.2 (3) ± 4.7	3 (2)	0.61	99.08
	1200	1780	Deep oxic water	3.3 (1)	3.29 (1)	0.48	99.72
M2	60	130–40	Oxic	4.7 (4) ± 1.9	na	na	na
	99	300–50	Oxycline	3 (5) ± 3.9	na	na	na
	102	130–100	Oxycline	1.4 (2)	na	0.94	99.02
	110	1300–10	Sec chl. max	7.7 (6) ± 3.5	11 (2)	2.8	97.94
	900	170–120	Deep oxic water	0.2 (2)	na	0.48	99.55
C1	5	900–10	Oxic	45 (16) ± 20.2	70 (1)	1.05	na
	30	900–400	Oxic	21.3 (4) ± 8.8	17(2)	0.31	na
	40	1300–30	Oxycline	15.5 (10) ± 5.1	17 (3) ± 3.6	0.17	na
	50	800–0	Below oxycline	12 (22) ± 6.1	16 (2)	0.13	na

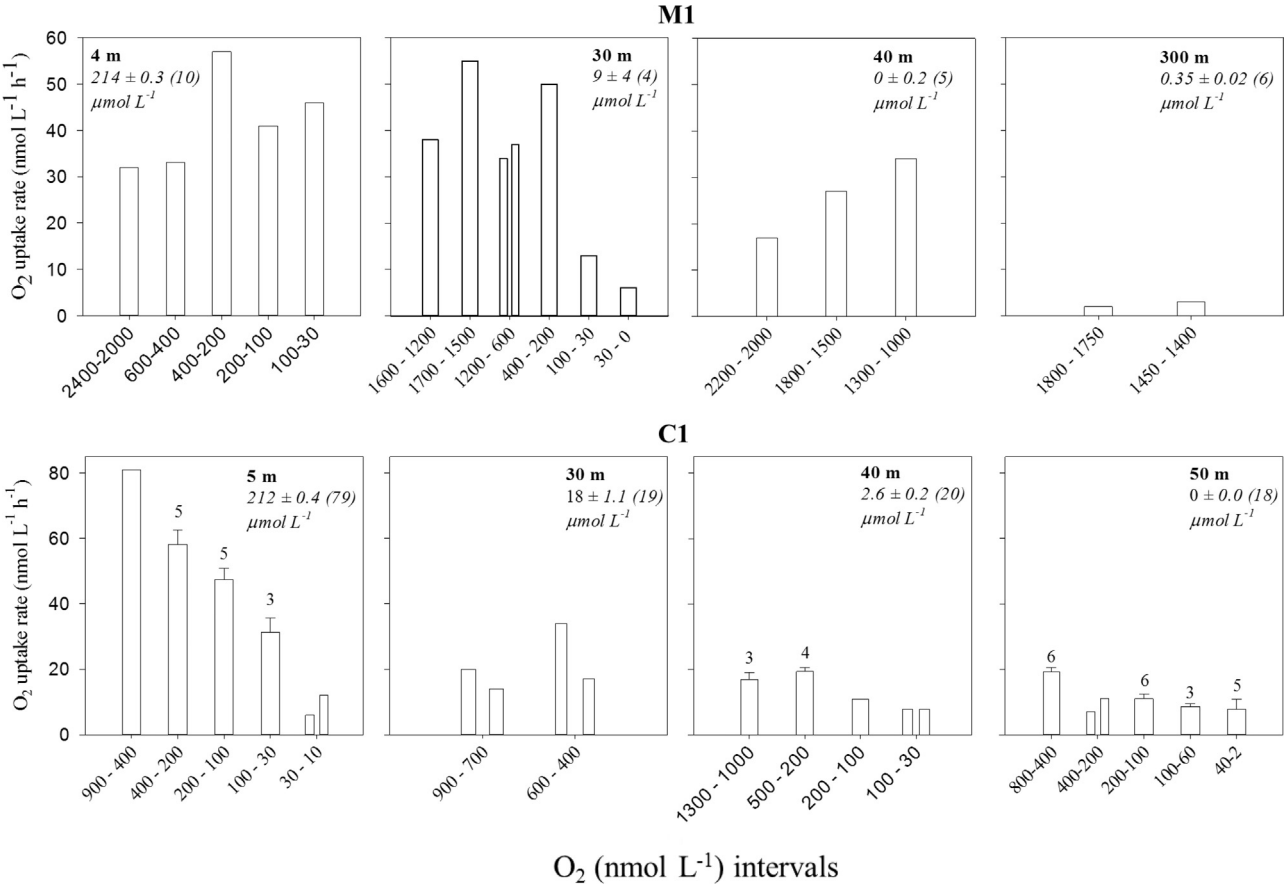

Fig. 4. *Community responses to variation in O_2 levels in incubation bottles.* Response of the planktonic communities, from different depths of St. M1 and St. C1, to variations in O_2 levels during the incubations. Sampling depths and in situ O_2 concentrations during the study period (average ± standard error (n)) are indicated by each graph. Note that for St. M1: 30 m corresponds to the oxycline, and 40 m to the secondary chlorophyll maximum; while for St. C1: 40 m corresponds to the oxycline. When duplicates were available both values were presented, when 3 or more replicates were available standard error was presented (n=3 to 7) on top of the graph's columns.

station, exhibited lower respiration rates than M1, in addition also here the rates correlated with fluorescence and turbidity peaks (R^2=0.9).

For Station C1 in the ETSP, CR started out with very high surface values (70 nmol O_2 L^{-1} h^{-1} at 5 m) and decreased along with the fluorescence with increasing depth (R^2=0.99). The rate

determinations for waters at oxycline depth (40 m) and shortly below (50 m), in anoxic waters, resulted in comparable values (17 nmol L^{-1} O_2 h^{-1}).

3.3.2. Community kinetics and response to different O_2 levels

Samples from both ETNP and ETSP OMZs were used to study the community response to different levels of O_2 (Table 2, Fig. 4). For Station M1, the planktonic community from surface waters (4 m) showed high O_2 uptake rates at all the analyzed O_2 levels (2.5–0 μmol L^{-1}). The apparent K_m value for this community, obtained by modeling the CR from a sample incubated in the 2–0 μmol L^{-1} O_2 range, was 113 nmol L^{-1} (model fit $R^2=0.998$). Instead in a parallel bottle, where the sampled water was incubated in the 500–0 nmol L^{-1} O_2 range, the apparent K_m value for the community was 18 nmol L^{-1} (model fit $R^2=0.996$). In both replicate samples the calculation of the K_m value was based on modeling of the 500–0 nmol L^{-1} O_2 depletion curve, according to the Jassby and Platt modified equation (Tiano et al., 2014).

The community inhabiting upper oxycline waters at M1 (25–30 m) behaved slightly differently and performed high respiration rates only above 100 nmol L^{-1} O_2. For samples below the upper oxycline, at 40 and 300 m depth, the potential for CR detected was relatively high (Table 2, column 2) considering the increasing depth and the in situ anoxic conditions.

Station C1 showed a different trend for surface waters (5 m) when considering rates at different O_2 concentration ranges; in fact CR seemed to decrease with O_2 in the concentration range 900–10 nmol L^{-1} (Fig. 4, for 5 m). When O_2 depletion curves from three different incubation bottles were modeled individually, we could, however, estimate quite low kinetic parameters for this community. In detail, data from the first bottle were modeled for the 1–0 μmol L^{-1} O_2 depletion curve, and they gave an apparent K_m value of 136 nmol L^{-1} (model fit $R^2=0.998$). Modeling of the 450–0 nmol L^{-1} O_2 depletion curve from the second bottle, gave an apparent K_m value of 69 nmol L^{-1} (model fit $R^2=1.000$). Last bottle, with modeling of the 400–0 nmol L^{-1} O_2 depletion curve, had an apparent K_m value was 107 nmol L^{-1} (model fit $R^2=0.995$). The average apparent K_m value ($\pm$SE) was 104 ± 19.5 ($n=3$) nmol L^{-1} O_2 (model fit $R^2=0.997 \pm 0.001$) with a V_{max} of 68 ± 9 ($n=3$) nmol L^{-1} h^{-1}.

The planktonic communities at C1 from low O_2 waters (30 m), oxycline (40 m) and anoxic (50 m) waters showed fairly constant respiration rates throughout the nanomolar range of concentrations. Due to the low respiration rates it was not possible to estimate reliable K_m values for these depths.

In incubations with water from the secondary chl. maximum at Station M2 (110 m), O_2 concentration decreased linearly in the range from 80–10 nmol L^{-1} O_2 (two reactors, data not shown).

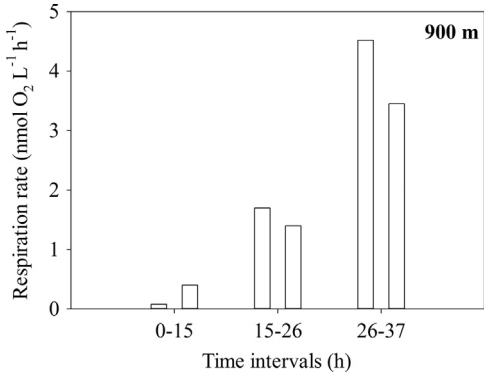

Fig. 5. *Effect of prolonged incubation time on the O_2 uptake rates.* Respiration rates expressed in duplicate bottles of 900 m water (Cast 170, Fig. 2) incubated over 37 h.

3.3.3. Community response to time and organic contamination

The influence of time and organic contaminations, accomplished by an addition of casamino acids, on respiration rates was investigated with two sets of incubations. For evaluating the effect of prolonged incubation time on community respiration in bottle incubations, water samples from 900 m depth at Cast 170 (Fig. 2) with presumably extremely low activity were incubated in two reactors for a total time of 37 h (Fig. 5). CR rates detected during the first 15 h were indeed very low (0.4–0.08 nmol L^{-1} h^{-1}), but they steadily increased to reach about 10 times the initial values in the time interval 26–37 h.

Another set of incubations lasting 58 h was performed with seawater from 102 m at St. M2, where the in situ O_2 concentration was 1 μmol L^{-1}. Duplicate bottles were set up with and without the addition of 1 mg L^{-1} of casamino acids (Fig. 6) to test the effect of increased dissolved organic matter concentration. Dissolved free amino acids (DFAA) are a source of both carbon and nitrogen, often constituting, even with concentrations in the low nanomolar range, a major proportion of the microbial C and N demands (Keil and Kirchman, 1999; Middelboe et al., 1995).

Initial (0–20 h) respiration rates for both treatments were very low: 1.6 and 1.9 nmol L^{-1} h^{-1}, for normal seawater and AA-treated seawater respectively. Over time rates increased, as for the 900 m water experiment just described, and after about 50 h the respiration rates in the unamended bottles were about 9 times higher than during the initial 20 h, whereas the rates in the amended bottles were about 33 times higher. Rates thus increased after 20 h of incubation due to uncharacterized bottle effect in unamended water, but the increase was much higher when easily degradable substrate such as amino acids were added. Oxic water had to be injected into the bottles to avoid anoxic conditions when the rate of consumption increased. Thus the rates of consumption were measured at O_2 concentrations decreasing from about 130 nmol L^{-1} to about 40 nmol L^{-1} during the first 40 h, and addition of O_2 saturated water then increased the concentration again to about 220 nmol L^{-1} after 40 h.

4. Discussion

4.1. OMZs and AMZs, in situ O_2 distribution

The in situ O_2 profiling of the ETNP OMZ, both in its coastal and oceanic areas, consistently showed O_2 levels below the detection limit of the STOX sensor, indicating the presence of a vast volume of functionally anoxic water (Figs. 2, 3, and S3). The presence of O_2 at low nanomolar levels (detection limit here down to <4 nmol L^{-1}) in OMZ core waters, which have residence times of several to tens of years (DeVries et al., 2012b), is unlikely to support any biological or

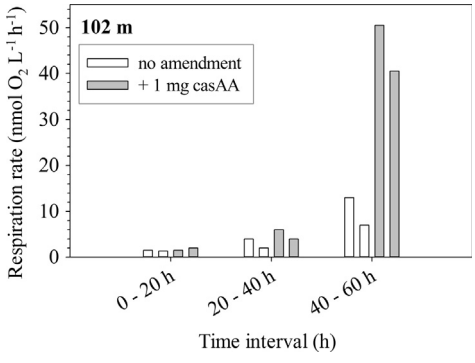

Fig. 6. *Effect of casamino acids additions on respiration rates in water from St. 2 at 102 m over a period of 60 h.* In white duplicates bottles with no amendment, in gray duplicate bottles with the addition of 1 mg L^{-1} of casamino acids.

biogeochemical aerobic processes. Knowing that the K_m values for high-affinity terminal oxidases may be only a few nmol L^{-1} (Morris and Schmidt, 2013), concentrations of 4 nmol L^{-1} would be reduced to the pmol L^{-1} level within relatively few hours, assuming V_{max} rates of 2–20 nmol L^{-1} h^{-1}, such as found near the upper oxycline. These results confirm the suggestion by Ulloa and colleagues (Ulloa et al., 2012), that the OMZ of the North Pacific could also be an AMZ since it features the same characteristic NO_2^- and N_2O profiles as the Arabian Sea (Jensen et al., 2011) and the ETSP OMZ (Thamdrup et al., 2012).

Similar conditions of undetectable O_2 were, at least for most of the experimental period, found for Station C1, which is a seasonal extension of the permanent ETSP OMZ (Montero et al., 2007). Station C1 is characterized by intrusion of nutrient-rich, oxygen-poor Equatorial Subsurface Waters (ESSW), which enhances primary productivity in the surface waters and subsequent organic matter degradation in subsurface waters. Pronounced changes in the depth of the oxycline occurred during the sampling period (Fig. 3), and the whole water body was actually oxic during the first two days of the experimental period. Detailed knowledge about the oxygen status of these waters, as presented in this paper, is critical in order to constrain models of elemental cycling and microbial activity.

4.2. OMZs and AMZs, planktonic community respiration

When the planktonic communities harboring these functionally anoxic waters are exposed to oxygen concentration at the nanomolar to few μmolar level (Tables 1 and 2), aerobic respiration starts immediately. This shows a high degree of versatility for microorganisms that are constantly exposed to, and most likely adapted to, anoxic conditions. It is possible that these communities maintain a functional machinery for aerobic metabolisms due to occasional mixing-events or intrusions of O_2-rich waters in the OMZ core (Whitmire et al., 2009). Signs of such an intrusion were found for Casts 170 (Fig. 2) and 171, where O_2 in sub-micromolar concentrations were found at about 500 m depth, separated from other oxic waters by hundreds of meters of anoxic water. Investigation of temperature and salinity profiles (Fig. S4) however did not show any sign of distinct water masses. This oxic water layer was also detected by the Seabird O_2 sensor (for a similar comparison of Seabird and STOX data see Fig. S1), confirming the validity of the measurement. Signs of turbulent mixing were found in the oxycline regions of the water column where O_2 profiles could be very irregular, but it is not clear how the nanomolar-oxic intrusion in the very core of the OMZ had happened. In order to draw down the O_2 concentration to below detection, and to keep it there, the microorganisms must be able to consume O_2 at these extremely low concentrations.

There are strong indications that the ability to respire O_2 in the lower nanomolar range is a common phenomenon in both natural communities and pure cultures of microorganisms (Lloyd, 2002; Stolper et al., 2010; Thamdrup, 2012; Tiano et al., 2014), and that branched respiratory chains give high metabolic flexibility to microorganisms; such as denitrifiers (Chen and Strous, 2013), which are mainly facultative, and would use oxygen first, if available (Zumft, 1997). The O_2 levels in the OMZs and O_2 affinity of aerobic processes, in combination with the sensitivity of anaerobic processes to O_2, control the distribution of these microbial processes. Nitrification requires O_2 but may proceed at very low O_2 concentrations (Bristow et al. unpubblished data, Lam et al., 2009; Martens-Habbena et al., 2009). Anammox and denitrification are traditionally considered to occur at O_2 concentrations up to 20 μmol L^{-1} (Devol, 1978; Jensen et al., 2011; Kalvelage et al., 2011; Kalvelage et al., 2013), but are now also suggested to be severely inhibited already at sub-micromolar O_2 concentrations (Dalsgaard et al., unpublished data, Babbin et al., 2014). The discrepancy between estimates of the O_2 sensitivity of dissimilatory nitrate and nitrite reduction may partially be due to differences in incubation conditions, where incubation in non-stirred water with aggregates may cause local oxygen depletion (e.g. Ploug, 2001). These conditions would allow anaerobic processes to occur under what appears to be relatively high O_2 concentrations, whereas incubation of water under stirred conditions may destroy aggregates and prevent local O_2 depletions, thus resulting in sensitivity concentrations and K_m estimates that might better reflect the physiology of the microorganisms.

4.2.1. Kinetics of planktonic community respiration

The CR of the analyzed water masses did in some cases exhibit pronounced changes with changes in O_2 concentration (Table 2 and Fig. 4), but seen as an average of the measured values for all locations there is very little O_2 dependence above O_2 concentrations of about 500 nmol L^{-1}, and the K_m values can thus in general be assumed to be below 250 nmol L^{-1}. Apparent K_m values for these mixed communities below 300–250 nmol L^{-1} are not surprising, as even the low affinity terminal oxidases have been reported to have K_m values in that range (Morris and Schmidt, 2013). Further Kalvelage and colleagues (Kalvelage et al., 2013) detected genes for high affinity terminal oxidases in the ETSP OMZ waters. It is likely that most prokaryotes living under electron donor limitation in deep low-oxygen Ocean water are fine-tuned to use the energetically most favorable electron acceptors available, as the diffusional supply of O_2 to the individual cell, even at concentrations of a few nanomolar, is sufficient to maintain the slow growth rates (Stolper et al., 2010) enabled by the low supply of electron donors. There are, however, also indications that the thermodynamically most feasible reactions may coexist with alternative reactions with less energy efficiency such as the occurrence of sulfate reduction in high-nitrate waters (Canfield et al., 2010).

Due to the low respiration rates in the deeper water layers of the open Ocean locations (C1 and M2) and the difficulties in getting initial O_2 concentrations sufficiently low only few incubations approached zero O_2 in <20 h. However, the two sets of data we have (from the secondary chlorophyll maximum of M2) suggest linearity of the O_2 depletion curve down to 20 nmol L^{-1} or less (linear regression between 60 and 10 nmol $L^{-1}$with $R^2=0.99$, and between 80 and 27 nmol $L^{-1}$with $R^2=0.97$). This may suggest K_m values of less than 10 nmol L^{-1}, but there may be two or more populations with very different K_m values in the same water layer. One of these populations might dominate respiration after changes in O_2 concentration and modeling of oxygen depletion curves over different concentration intervals may thus result in different kinetic parameters.

For surface waters (4 m) of Station M1, different apparent K_m values (113 nmol L^{-1} vs 18 nmol L^{-1}, see Section 3.3.2) were obtained by modeling two depletion curves over the same O_2 range. The two depletion curves correspond to two replicate samples which were incubated at two different concentration ranges: 2–0 and 500–0 nmol L^{-1} O_2 respectively. A simple Michaelis–Menten (or Jassby and Platt) model is thus an oversimplification. Where there is a significant contribution of high-affinity terminal oxidases we may thus expect a near-constant rate of decrease in O_2 in about 80–10 nmol L^{-1} range (assuming a K_m of 3 nmol L^{-1} for the high-affinity terminal oxidases) and above 500 nmol L^{-1} (assuming a K_m for the low affinity terminal oxidases of 200 nmol L^{-1}).

The scatter in CR values presented in Table 2 and Fig. 4 can to a major extent be explained by the natural variability among replicate bottles filled from a common larger reservoir, where one single crushed aggregate or a larger eukaryote may significantly affect the activity within a single bottle.

The ability to efficiently respire very low O_2 concentrations could be expected for the secondary chl. maximum layers of the

OMZ, where a tight coupling between O_2 producing cyanobacteria, especially of the genus *Prochlorococcus* (Goericke et al., 2000; Lavin et al., 2010), and organic matter degradation through aerobic processes is likely taking place. In some profiles we detected sub-micromolar O_2 concentrations in the secondary chlorophyll layer (Fig. 3, Fig. S4), indicating that the photosynthetic activity might contribute to a rather thick (~10 m) water layer with these low O_2 concentrations. Low but sufficient blue light was previously detected in the ETNP OMZ in correspondence with the secondary chl. maximum (Cepeda-Morales et al., 2009). Similarly, in our study, the photosynthetically active radiation (PAR) in the secondary chlorophyll maximum (i.e. Cast 147) was comparable to 1.3% of the PAR present in the first chlorophyll maximum (see results in Section 3.2). Therefore there may be a significant volume of water within the secondary chlorophyll layer that shift between oxic conditions and functional anoxia during diurnal light cycles. A respiration rate of 7.7 nmol L^{-1} h^{-1} would thus suffice to make water with initially 48 nmol L^{-1} O_2, functionally anoxic during a 12 h dark period. In those cases, where we did not detect O_2 in the secondary chlorophyll maximum there may have been a tight coupling between simultaneously ongoing aerobic and anaerobic processes at the vanishingly low O_2 concentrations that can be expected to be present during the light hours. It still needs to be elucidated which ones are the oxic and anoxic processes that occur in actively photosynthesizing, and thus O_2 producing, secondary chlorophyll maxima, when O_2 is below the detection limit.

4.2.2. Regional and depth variation of CR

Respiration rates were higher at the more productive coastal Stations (M1, C1) than at the open Ocean Station (M2). Oxygen uptake was higher in surface and subsurface layers, coinciding with higher chlorophyll concentrations and lower beam transmission values (Table 2) indicating that higher respiration rates were connected to higher densities of phytoplankton and microorganisms and/or suspended particles. Although respiration rates generally decrease with depth (Feely et al., 2004; Karstensen et al., 2008), we observed relatively high activities in waters at the oxycline. Relatively high rates of potential respiration were also measured in the originally anoxic waters just below the oxic–anoxic interface when these were incubated at low oxygen concentrations (Table 2, M1: 30–40 m, C1: 40–50 m). These zones are characterized by high rates of re-mineralization, which lead to OMZ intensification, and aerobic and anaerobic processes in these layers may occur simultaneously under nanomolar-oxic conditions (Thamdrup, 2012), or just temporally separated due to oxygen intrusions or photosynthetic activity. The oxic–anoxic interface may thus be a site for intensive oxidation of NO_2^- that accumulate to relatively high concentrations (Thamdrup, 2012) in the anoxic water masses. This O_2-requiring process may co-occur with anaerobic processes such as NO_3^- reduction to NO_2^- which seems to be less inhibited by O_2 than other N-reducing processes (Kalvelage et al., 2011, 2013).

4.3. Community response to time and organic contamination

Direct assessments of the very low microbial respiration below 200 m in the water column are rare and results are controversial (Arístegui et al., 2005a, 2005b; Reinthaler et al., 2006), despite the fact that those water masses account for 72% of the volume of the global Ocean.

Our method was able to resolve respiration rates even below 200 m depth, during incubations of <15 h. Due to the STOX sensor's very low detection limit, oxygen uptake rates down to ~0.02 μmol L^{-1} O_2 d^{-1} at O_2 concentrations of about 100 nmol L^{-1} could be determined.

Respiration rates measured after more than 20 h of incubation were greatly overestimated (Fig. 5), and did not reflect the original metabolic activity of the planktonic community, possibly due to "bottle effects" (Robinson and Williams, 2005; Sherr et al., 1999; Stewart et al., 2012). There is, of course, also a possibility for overestimation of metabolic rates during the initial 20 h, due to possible contaminations with organic material from the sampling and incubation equipment. We tested this possibility by adding casamino acids (Fig. 6) and observed no significant increase in respiration within the first 20 h. The addition had the potential to stimulate respiration, as highly increased rates were observed after 20 h. However, the dominating bacterial population in this open Ocean sample was apparently not geared to take immediate advantage of the increased nutrient availability. Dominating groups of free-living cells in the oligotrophic Ocean such as the SAR11 cluster are reported to be very limited in metabolic potential (Grote et al., 2012) and might not be able to respond immediately to increased nutrient concentrations. However, gene expression analysis indicates that they respond to sampling and laboratory incubation with a pronounced stress response (Stewart et al., 2012).

5. Conclusions

To conclude we have here reported oxygen distributions associated with the north and south east Pacific OMZs core regions to be below detection limits. Considering the presence of high-affinity terminal oxidases, with K_m values of about 3 nmol L^{-1} that would reduce concentrations of a few nanomolar to femtomolar levels in a few hours, these layers can be defined as functionally anoxic.

We have also quantified the O_2 consumption and its kinetics, by relying on multiple STOX sensors functioning simultaneously. Our measurements have been limited to few replicates due to a limited numbers of functioning sensors, but we have been able to demonstrate the general distribution of oxic metabolism and its kinetics throughout the water column. The very low consumption rates of <5 nmol L^{-1} h^{-1} could only be reliably resolved at O_2 concentrations below about 200 nmol O_2, with a detection limit of about 0.5–1 nmol L^{-1} h^{-1}. Advances in electrochemical sensor and optode technology (Holtappels et al., 2014; Koren et al., 2013) will no doubt considerably lower this detection limit and it is our estimate that we in the future will be able to reliably determine rates down below 0.1 nmol L^{-1} h^{-1}.

Another limitation has been the assumption of a fair description of O_2 uptake kinetics by Michaelis–Menten or modified Michaelis–Menten (i.e. Jassby and Platt) models. These models do not strictly apply to mixed communities, but better alternatives are lacking.

The O_2 respiration rates found near the oxic-anoxic interface (2–30 nmol L^{-1}) are generally one order of magnitude higher than combined denitrification and anammox rates reported from similar or same locations (e.g., Dalsgaard et al., 2012; Hamersley et al., 2007; Kalvelage et al., 2013). However, some of these rates may be underestimated, possibly due to O_2 present in the incubations. This O_2 contamination may originate from polymers in Niskin bottles and rubber septa (De Brabandere et al., 2012).

Respiration rates should preferably be measured during incubations lasting less than 16 h as we found pronounced increases in respiration rates, that we could only attribute to effects of the enclosure (i.e. bottle effects), in longer incubations. These bottle effects may have caused some of the inconsistencies in the O_2 budgets based on previously collected data (Biddanda and Benner, 1997), as the low activity in Ocean water has required long incubation times by the methods applied until now. There are still many unanswered questions about the transformations in OMZ regions, and many of these questions are associated with the

impact of sub-micromolar O_2 concentrations on the actual biogeochemical transformations. We now have significantly improved tools to elucidate these interactions.

Acknowledgments

We greatly acknowledge Preben G. Sørensen and Lars B. Pedersen for their technical assistance and Justyna Jonca for testing the temperature dependence of the STOX sensors. Special thanks to Gadiel Alarcón, and all crew members of the R/V Kay Kay, and R/V Thomas G. Thompson for their efficient assistance during our work on board, and Aaron Morello for doing onboard chemical analyses. This study was supported by the Danish Natural Science Research Council, Grant no. 10-083140, the European Research Council, Grant no. 267233, the Gordon and Betty Moore Foundation, and the Agouron Institute. Osvaldo Ulloa was supported by the Millennium Scientific Initiative, IC 120019

Appendix A. Supporting information

Supplementary data associated with this article can be found in the online version at http://dx.doi.org/10.1016/j.dsr.2014.10.001.

References

Arístegui, J., Agustí, S., Middelburg, J.J., Duarte, C.M., 2005a. Respiration in the mesopelagic and bathypelagic zones of the Oceans. In: Giorgio, P.D., Williams, P. (Eds.), Respiration in Aquatic Ecosystems. Oxford University Press, Oxford, pp. 181–205.

Arístegui, J., Duarte, C.M., Gasol, J.M., Alonso-Saez, L., 2005b. Active mesopelagic prokaryotes support high respiration in the subtropical northeast Atlantic Ocean. Geophys. Res. Lett. 32, 3.

Babbin, A.R., Keil, R.G., Devol, A.H., Ward, B.B., 2014. Organic matter stoichiometry, flux, and oxygen control nitrogen loss in the Ocean. Science.

Bange, H.W., 2006. Nitrous oxide and methane in European coastal waters. Estuar. Coast. Shelf Sci. 70 (3), 361–374.

Biddanda, B., Benner, R., 1997. Major contribution from mesopelagic plankton to heterotrophic metabolism in the upper Ocean. Deep Sea Res. Part I: Oceanogr. Res. Pap. 44 (12), 2069–2085.

Canfield, D.E., Stewart, F.J., Thamdrup, B., De Brabandere, L., Dalsgaard, T., Delong, E.F., Revsbech, N.P., Ulloa, O., 2010. A cryptic sulfur cycle in oxygen-minimum–zone waters off the Chilean coast. Science 330 (6009), 1375–1378.

Cepeda-Morales, J., Beier, E., Gaxiola-Castro, G., Lavín, M., Godínez, V., 2009. Effect of the oxygen minimum zone on the second chlorophyll maximum in the Eastern Tropical Pacific off Mexico Efecto de la zona del mínimo de oxígeno en el segundo máximo de clorofila en el Pacífico Oriental Tropical Mexicano. Ciencias Marinas 35 (4), 389–403.

Chen, J., Strous, M., 2013. Denitrification and aerobic respiration, hybrid electron transport chains and co-evolution. Biochim. et Biophys. Acta (BBA) – Bioenerg. 1827 (2), 136–144.

Dalsgaard, T., Thamdrup, B., Farias, L., Revsbech, N.P., 2012. Anammox and denitrification in the oxygen minimum zone of the eastern South Pacific. Limnol. Oceanogr. 57 (5), 1331–1346.

De Brabandere, L., Thamdrup, B., Revsbech, N.P., Foadi, R., 2012. A critical assessment of the occurrence and extend of oxygen contamination during anaerobic incubations utilizing commercially available vials. J. Microbiol. Methods 88 (1), 147–154.

Devol, A.H., 1978. Bacterial oxygen uptake kinetics as related to biological processes in oxygen deficient zones of the Oceans. Deep-Sea Res. 25, 137–146.

DeVries, T., Deutsch, C., Primeau, F., Chang, B., Devol, A., 2012a. Global rates of water-column denitrification derived from nitrogen gas measurements. Nat. Geosci. 5 (8), 547–550.

DeVries, T., Primeau, F., Deutsch, C., 2012b. The sequestration efficiency of the biological pump. Geophys. Res. Lett. 39 (13), L13601.

Feely, R.A., Sabine, C.L., Schlitzer, R., Bullister, J.L., Mecking, S., Greeley, D., 2004. Oxygen utilization and organic carbon remineralization in the upper water column of the Pacific Ocean. J. Oceanogr. 60 (1), 45–52.

Glud, R.N., Gundersen, J.K., Ramsing, N.B., 2000. Electrochemical and optical oxygen microsensors for in situ measurements. In in situ monitoring of aquatic systems: Chemical analysis and speciation. John Wiley & Sons Ltd (eds Buffle, J., Horvai, G.). Chapter 2:19-73.

Goericke, R., Olson, R.J., Shalapyonok, A., 2000. A novel niche for Prochlorococcus sp in low-light suboxic environments in the Arabian Sea and the Eastern Tropical North Pacific. Deep-Sea Res. Part I-Oceanogr. Res. Pap. 47 (7), 1183–1205.

Grote, J., Thrash, J.C., Huggett, M.J., Landry, Z.C., Carini, P., Giovannoni, S.J., Rappe, M.S., 2012. Streamlining and core genome conservation among highly divergent members of the SAR11 Clade. MBio 3, 5.

Hamersley, M.R., Lavik, G., Woebken, D., Rattray, J.E., Lam, P., Hopmans, E.C., Damsté, J.S., Kruger, S., Graco, M., Gutiérrez, D., 2007. Anaerobic ammonium oxidation in the Peruvian oxygen minimum zone. Limnol. Oceanogr. 52 (3), 923.

Holtappels, M., Tiano, L., Kalvelage, T., Lavik, G., Revsbech, N.P., Kuypers, M.M.M., 2014. Aquatic respiration rate measurements at low oxygen concentrations. PLoS One 9 (2), e89369.

Jassby, A.D., Platt, T., 1976. Mathematical formulation of relationship between photosynthesis and light for phytoplankton. Limnol. Oceanogr. 21 (4), 540–547.

Jensen, M.M., Lam, P., Revsbech, N.P., Nagel, B., Gaye, B., Jetten, M.S.M., Kuypers, M.M.M., 2011. Intensive nitrogen loss over the Omani Shelf due to anammox coupled with dissimilatory nitrite reduction to ammonium. ISME J. 5 (10), 1660–1670.

Kalvelage, T., Jensen, M.M., Contreras, S., Revsbech, N.P., Lam, P., Gunter, M., LaRoche, J., Lavik, G., Kuypers, M.M.M., 2011. oxygen sensitivity of anammox and coupled n-cycle processes in oxygen minimum zones. PLoS One 6, 12.

Kalvelage, T., Lavik, G., Lam, P., Contreras, S., Arteaga, L., Loscher, C.R., Oschlies, A., Paulmier, A., Stramma, L., Kuypers, M.M.M., 2013. Nitrogen cycling driven by organic matter export in the South Pacific oxygen minimum zone. Nat. Geosci. 6 (3), 228–234.

Karstensen, J., Stramma, L., Visbeck, M., 2008. Oxygen minimum zones in the eastern tropical Atlantic and Pacific Oceans. Prog. Oceanogr. 77 (4), 331–350.

Keeling, R.F., Kortzinger, A., Gruber, N., 2010. Ocean deoxygenation in a warming world. Annu. Rev. Mar. Sci., 199–229 (Palo Alto).

Keil, R.G., Kirchman, D.L., 1999. Utilization of dissolved protein and amino acids in the northern Sargasso Sea. Aquat. Microb. Ecol. 18, 293–300.

Koren, K., Hutter, L., Enko, B., Pein, A., Borisov, S.M., Klimant, I., 2013. Tuning the dynamic range and sensitivity of optical oxygen-sensors by employing differently substituted polystyrene-derivatives. Sens. Actuators B: Chem. 176 (0), 344–350.

Lam, P., Lavik, G., Jensen, M.M., van de Vossenberg, J., Schmid, M., Woebken, D., Gutiérrez, D., Amann, R., Jetten, M.S.M., Kuypers, M.M.M., 2009. Revising the nitrogen cycle in the Peruvian oxygen minimum zone. Proc. Natl. Acad. Sci. 106 (12), 4752–4757.

Lavin, P., González, B., Santibáñez, J.F., Scanlan, D.J., Ulloa, O., 2010. Novel lineages of Prochlorococcus thrive within the oxygen minimum zone of the eastern tropical South Pacific. Environ. Microbiol. Rep. 2 (6), 728–738.

Lloyd, D., 2002. Noninvasive methods for the investigation of organisms at low oxygen levels In: Allen I. Laskin, J.W.B., Geoffrey, M.G. (Eds.), Advances in Applied Microbiology. Academic Press, pp. 155–184e.

Martens-Habbena, W., Torre, R, De Stahl, D.A., Berube, P.M., Urakawa, H., 2009. Ammonia oxidation kinetics determine niche separation of nitrifying Archaea and Bacteria. Nature.

Middelboe, M., Borch, N., Kirchman, D., 1995. Bacterial utilization of dissolved free amino acids, dissolved combined amino acids and ammonium in the Delaware Bay estuary: effects of carbon and nitrogen limitation. Mar. Ecol. Prog. Ser. 128, 109–120.

Montero, P., Daneri, G., Cuevas, L.A., Gonzalez, H.E., Jacob, B., Lizarraga, L., Menschel, E., 2007. Productivity cycles in the coastal upwelling area off Concepcion: The importance of diatoms and bacterioplankton in the organic carbon flux. Prog. Oceanogr. 75 (3), 518–530.

Morris, R.L., Schmidt, T.M., 2013. Shallow breathing: bacterial life at low O_2. Nat. Rev. Micro. 11 (3), 205–212, http://dx.doi.org/10.1038/nrmicro2970.

Paulmier, A., Ruiz-Pino, D., 2009. Oxygen minimum zones (OMZs) in the modern Ocean. Prog. Oceanogr. 80 (3–4), 113–128.

Ploug, H., 2001. Small-scale oxygen fluxes and remineralization in sinking aggregates. Limnol. Oceanogr. 46, 1624–1631.

Reinthaler, T., van Aken, H., Veth, C., Aristegui, J., Robinson, C., Williams, P.J.L.R., Lebaron, P., Herndl, G.J., 2006. Prokaryotic respiration and production in the meso- and bathypelagic realm of the eastern and western North Atlantic basin. Limnol. Oceanogr. 51 (3), 1262–1273.

Revsbech, N.P., Larsen, L.H., Gundersen, J., Dalsgaard, T., Ulloa, O., Thamdrup, B., 2009. Determination of ultra-low oxygen concentrations in oxygen minimum zones by the STOX sensor. Limnol. Oceanogr.: Methods 7, 371–381.

Revsbech, N.P., Thamdrup, B., Dalsgaard, T., 2011. Construction of STOX oxygen sensors and their application for determination of o_2 concentrations in oxygen minimum zones. Methods Enzymol. 486, 325–341.

Robinson, C., Williams, P.J.l.B., 2005. Respiration and its measurement in surface marine waters. In: Giorgio, P.D, Williams, P (Eds.), Respiration in Aquatic Ecosystems. Oxford University Press, Oxford, pp. 147–180.

Schmidt, J., 1925. On the contents of oxygen in the Ocean on both sides of panama. Science 61 (1588), 592–593.

Sherr, E.B., Sherr, B.F., Sigmon, C.T., 1999. Activity of marine bacteria under incubated and in situ conditions. Aquat. Microb. Ecol. 20, 213–223.

Stewart, F.J., Dalsgaard, T., Young, C.R., Thamdrup, B., Revsbech, N.P., Ulloa, O., Canfield, D.E., DeLong, E.F., 2012. Experimental incubations elicit profound changes in community transcription in omz bacterioplankton. PLoS ONE 7 (5), e37118.

Stolper, D.A., Revsbech, N.P., Canfield, D.E., 2010. Aerobic growth at nanomolar oxygen concentrations. Proc. Natl. Acad. Sci. USA 107, 18755–18760.

Stramma, L., 2008. Expanding oxygen-minimum. Science, 655.

Thamdrup, B., 2012. New pathways and processes in the global nitrogen cycle. Annu. Rev. Ecol. Evol. Syst. 43 (1), 407–428.

Thamdrup, B., Dalsgaard, T., Revsbech, N.P., 2012. Widespread functional anoxia in the oxygen minimum zone of the Eastern South Pacific. Deep Sea Res. Part I: Oceanogr. Res. Pap. 65, 36–45.
Tiano, L., Garcia-Robledo, E., Revsbech, N.P., 2014. A new highly sensitive method to assess respiration rates and kinetics of natural planktonic communities by use of the switchable trace oxygen sensor and reduced oxygen concentrations. PLoS One 9 (8), e105399.
Ulloa, O., Canfield, D.E., DeLong, E.F., Letelier, R.M., Stewart, F.J., 2012. Microbial Oceanography of anoxic oxygen minimum zones. Proceedings of the National Academy of Sciences 109, 15996–16003.
Whitmire, A.L., Letelier, R.M., Villagran, V., Ulloa, O., 2009. Autonomous observations of in vivo fluorescence and particle backscattering in an oceanic oxygen minimum zone. Opt. Express 17 (24), 21992–22004.
Wright, J.J., Konwar, K.M., Hallam, S.J., 2012. Microbial ecology of expanding oxygen minimum zones. Nat. Rev. Microb. 10, 381–394.
Wyrtki, K., 1962. The oxygen minima in relation to Ocean circulation. Deep Sea Res. Oceanogr. Abstr. 9 (1–2), 11–23.
Zumft, W., 1997. Cell biology and molecular basis of denitrification. Microbiol. Mol. Biol. Rev., 533–616.